Electron impact ionization of 1-propanol

Electron Impact Ionization of 1-Propanol

W. A. D. Pires[1], K. L. Nixon[1,2], S. Ghosh[1], R. F. C. Neves[1,3], H. V. Duque[1], R. A. A. Amorim[1], D. B. Jones[4], F. Blanco[5], G. Garcia[5], M. J. Brunger[4] and M. C. A. Lopes[1 *]

[1] Departamento de Física, Universidade Federal de Juiz de Fora, Juiz de Fora, MG, 36936-900, Brazil
[2] Wolverhampton School of Sciences, University of Wolverhampton, Wolverhampton WV1 1LY, UK
[3] Instituto Federal do Sul de Minas Gerais, Campus Poços de Caldas, Minas Gerais, Brazil
[4]School of Chemical and Physical Sciences, Flinders University, GPO Box 2100, Adelaide SA 5001, Australia
[5] Instituto de Física Fundamental, Consejo Superior de Investigaciones Científicas (CSIC), Serrano 113-bis, 28006 Madrid, Spain

* corresponding author: cristina.lopes@ufjf.edu.br

Abstract

Experimental measurements of the cations created in electron impact ionization have been undertaken for the primary isomer of propanol using a Hidden Quadrupole Mass Spectrometer (EPIC 300), with a mass resolution of 1 amu. The mass spectra recorded at an incident electron energy of 70 eV reveals the relative probability of forming 50 different cations, by either direct ionization or dissociative ionization. Individual partial ionization cross sections (PICS) for 31 different cations were measured for the first time in this work, for the incident electron energy range from 10 to 100eV. Also, appearance energies (AEs) and Wannier exponents for the 16 most intense cations formed in electron collisions with 1-propanol are reported. Where possible, those results are compared to those from an earlier investigation. Total Ionization Cross Sections (TICS) were also obtained from the sum of the measured PICS, for nearly all cations measured, and are compared to relevant data reported in the literature. In addition, as a part of this study, theoretical TICS were calculated using the Binary-encounter Bethe (BEB) and independent atom model with screening corrected additivity rule (IAM - SCAR) methods. Good agreement between current measured and calculated TICSs and corresponding earlier results was typically found.

PACS numbers: 34.80.Ht, 34.80.Gs

1. Introduction

In an era of globalization, which is marked by a rapid expansion in industrialization, the indiscriminate use of petroleum-based fuels is the object of many discussions. These discussions have observed that those resources are finite, are rapidly decreasing, and their price is steeply increasing [1-2]. Furthermore, their intensive use in many areas produces environmental degradation [3], which probably leads to climate change and global warming [1]. As a result, in order to control the demand for fossil fuels and to reduce the environmental hazards, governmental and industrial sectors are giving tremendous attention into research that uses bio-origin fuels as potential alternative energy sources [4]. The chemical and biological synthetization, and studies of their thermodynamic properties, of the first four aliphatic alcohols (methanol, ethanol, propanol and butanol) indicates some features that suggest they might be used in internal combustion engines [5-6]. However, these alternative alcohol fuels must initially be better understood and optimized, in order to realize their most efficient operating conditions, in such engines for complete combustion and highest energy release [7]. In the internal combustion engine, the ignition of a plasma [8] and also the residual products created by that plasma, such as positive ions, can be characterized by their Total and Partial Ionization Cross Sections (TICS and PICS). The accurate determination of the cations formed and also their ionization and fragmentation energies, namely the Ionization Energies (IE) and Appearance Energies (AEs), is an important basis for an understanding of many electron impact phenomena, such as the processes present in an ignition system.

Electron impact ionization is a phenomenon that can be efficiently investigated using mass spectrometry, which may produce new information not only about the variety of the cations formed but also reveal their Total and Partial ICSs. [9]. Although for a few decades researchers have been studying electron impact ionization of atoms and molecules, there is still much to be done in order to have a complete and reliable data base for many molecules. Indeed, up to now, absolute ICS for all energetically open scattering channels have been measured for only a very few molecules [10]. There has been a significant amount of studies for electron impact of methanol and ethanol, as was noted in Ref. [9] and references therein. Theoretical and experimental investigations of the Total Ionization Cross Sections for electron impact were reported by references [9, 11-17], while Partial Ionization Cross Sections were reported by references [9, 14-18]. Appearance energies (AEs) for methanol and ethanol were much less studied, and were reported by only a few authors [9, 18-20]. Nonetheless, these studies have produced important information for modeling the use of those alcohols as biofuels. However, there is not much information in the literature on electron collisions with 1-propanol [12-14, 18, 21- 24]. Khakoo *et al.* [21] reported experimental and calculated differential cross sections for elastic scattering of low energy electrons by 1-propanol, for selected impact energies ranging from 1 to 100eV. Their measurements were carried out using the relative-flow method, and the calculations employed two different implementations of the Schwinger multichannel variational method including polarization effects. Hudson e*t al.* [14] reported experimental and calculated absolute TICSs for propanol, for electron impact energies ranging from 16 to 200 eV and for all its isomers. Their experimental data were obtained using a linear transmission apparatus, while the

calculated results were obtained using a Deutsch–Märk (DM) additivity method, the Binary Encounter Bethe (BEB) method and a polarisation model. More recently, Bull *et al.* [23] reported theoretical absolute total electron impact ionization cross-section data, and polarizability parameters, for 65 polyatomic molecules, including 1- propanol. Their data were produced using the empirical polarizability correlation and BEB models, and the functional group additivity approximation. Takeuchi *et al*. [24] investigated the fragmentation mechanisms of 1-propanol by low energy electron impact, specifically for energies in the range 8-25 eV, and also generated potential energy curves calculated using *ab initio* MO methods. Beside that theoretical study, their 1-propanol experimental work used a Hitachi RMU-6M mass spectrometer to obtain total positive ion abundances. Rejoub *et al.* [18] measured absolute partial and total cross sections, for electron-impact ionization of 1-propanol from threshold to 1000 eV, for groups of cations with similar mass, by using a time-of-flight mass spectrometer. Finally, Williams and Hamill [22] measured AEs and bond dissociative energies for 1-propanol using a retarding potential difference (RPD) method in their mass spectrometer. They found the onsets for production of the $C_3H_7O^+$ cation (m=59 amu) at 10.93 eV and a slope change at 14.07 eV.

This paper is an extension of our previous work [9], where we investigated electron impact ionization of methanol and ethanol. We report here a study of electron impact ionization and ionic fragmentation of 1-propanol, using mass spectroscopy, where we measured for the first time the PICS for individual ionic fragments, over the energy range 10-100 eV. Adding up the PICS, which were normalized to an absolute scale, we also obtained an absolute TICS. Corresponding theoretical BEB and IAM – SCAR TICS were also calculated as a part of this study. In addition, AEs for a range of cations formed in electron collisions with 1-propanol are reported. The mass spectrum obtained reveals the relative probability of forming the various cation fragments by either direct ionization, as well as dissociative ionization, using incident electrons of 70 eV. For many of the mass values more than one cation fragment is possible, thus making the assignment of each peak observed a little more difficult. In these cases, the appearance energy helps us to determine the identity of the fragments recorded. Finally, PICS for a group of cations of 1-propanol were compared to the only previously published data from Rejoub *et al.* [18].

The structure of the remainder of this paper is as follows. In Section 2 we describe the experimental methods and analysis procedures, and our theoretical TICS calculations, while in Section 3 the mass spectra, PICS and TICS, as well as the AEs we determined are presented and discussed. Finally, some conclusions from this investigation are summarised in Section 4.

2. Experimental methods, analysis procedures and theory details

The experimental apparatus has been described in some detail in a previous article [9], so that only a brief description need be given here. The electron impact ionization experiments with 1-propanol have been performed using a Hiden Analytical [25] quadrupole mass spectrometer (QMS), fitted with a RF head capable of measuring masses up to 300 amu (EPIC 300) and with 1 amu

resolution. This apparatus has an ionization stage and so can be operated in a residual gas analysing (RGA) mode, which was applied in this work. The internal ionization source is used to create ions by electron impact ionization. The ions created are most likely to arise from the uniform background of target molecules, which effused from a needle positioned perpendicular to the axis of the mass filter and below the entrance to the ionization stage. In these studies an electron current of 20 μA and operating pressures of 1–1.5 × 10^{-6} Torr were used. No mass dependence of the QMS over the mass range studied in this work was found, as was investigated in some detail in our previous work [9]. The behavior of our apparatus was checked by measurements of the PICS for Argon, Ar^+, over the energy range from 10-100eV. That data was compared to the corresponding results from Rejoub *et al.* [26], obtaining excellent agreement [9], thereby demonstrating that appropriate tuning of all the parameters of the spectrometer had been achieved.

The samples of 1-propanol were degassed by several freeze-pump-thaw cycles before the vapour was admitted into the chamber using a needle valve (MLV-22 [27]). The gas handling lines were heated to ~ 40°C, to prevent condensation of the vapour along the lines, and so yield a stable operating pressure, although the vacuum vessel itself did not require heating and remained at the temperature of the air-conditioned laboratory, *i.e.*, 22°C. The vapour pressure of 1-propanol was calculated to be 17.39 torr, using the Antoine Equation [9], where the constants employed were A = 5.31384, B = 1690.864 and C = -51.804 [28].

The mass spectra for 1-propanol, as well as the residual background, were recorded on several separate days spanning this study. After the background signal was subtracted from the mass spectra, the average spectrum was normalised to the most intense peak. The results from this process are shown in figure 1 and table 1. The standard deviation on the relative cations abundances were determined after that normalization process. The recorded mass spectrum at 70 eV, as well as the PICS at 70eV, were set on an absolute scale, using the sum of the PICS for the various groups of cations corresponding to those reported by Rejoub *et al.* [18]. Note that the absolute data of Rejoub *et al.* at 70 eV was determined by an interpolation of the data they reported at 60 eV and 80 eV. The error bars in our mass spectrum and in the PICS were obtained by the mean square root of the square of the statistical error on our measurements, added to the square of the total error of the Rejoub *et al.* [18] measurements. A sum of the absolute PICS for all the cations subsequently yields the absolute TICS, with its errors being the mean square root of the square of statistical errors as well as inheriting the uncertainty in the absolute measurements of Rejoub *et a*l. [18] that we used in the normalization.

The production of ion fragments as a function of the incident electron energy can be described by the Wannier Law (equation 1). From measurements of near-threshold PICS curves, the ionization energy of the parent ion and the AEs of the others cation fragments can be obtained as fitting parameters of the Wannier Law, convoluted with the experimental instrument response function. Here we employ a Gaussian function as the instrument response function to represent the electron energy spread or resolution of the incident electron beam. Note that the

energy spread (resolution) arises from the thermionic emission of electrons from the filament, with the convolution used in our analyses of the PICS being given by (equation 2) [29,30]:

$$f(E) = \begin{matrix} 0 & E < AE \\ A(E - AE)^p & E \geq AE. \end{matrix} \quad (1)$$

$$f'(E) = \int_{AE}^{\infty} \frac{-(E-E_0)^2}{2\sigma^2} A(E_0 - AE)^p dE_0 \quad (2)$$

In equations (1) and (2), *AE* is the appearance energy, *p* is the Wannier exponent, *A* is a scaling factor, σ is the full-width-half-maximum (FWHM) of the Gaussian function, related to the spread of the incident electron beam (ΔE), where ΔE = 2.35 σ [31]. The fitting was performed using Origin Pro 9.1, with a non-linear fit employing the Marquart-Levenberg algorithm.

The analysis procedures described in this work are different to that employed by Nixon *et al.* [9] and we believe it is more physical. Having said that, however, when we applied both the present and the earlier [9] procedures to our 1-propanol results, differences in the determined PICS, TICS and AEs were always less than 2% which is not significant. Employing the present procedure, the AE of argon (15.759 eV) was used to calibrate the energy scale of our mass spectra and the PICS curves, as well as to determine the energy resolution of the electron beam. Assuming the Wannier exponent, *p,* of argon is 1.35 [29], the equation (2) can be fitted to the experimental argon data with *p* being a fixed parameter and the value of σ a variable of the fit. It should be mentioned that we did not use the proposed value of p = 1.27 ± 0.05 reported by Gstir *et al.* [32], given that the value of 1.35 produced better fits to our experimental data and generated values of the argon AEs which are in better agreement with data from the literature, where such a comparison was possible. Using this procedure, we have obtained the energy resolution of our electron beam to be ~ 660 meV, when using data up to 2 eV above the AE, corresponding to σ = 0.28 eV. This value was subsequently used as a fixed parameter in the fitting procedure of our near-threshold experimental 1-propanol PICS data, in order to obtain the AEs for 1-propanol, as shown in the table 2. The errors on the determination of AEs for 1-propanol are given by the fitting procedures using the Marquart-Levenberg algorithm. Note that table 2 also includes a selection of recommended 1-propanol AE values from NIST [33].

As a part of present investigation, TICS were calculated within the BEB formalism [34] and the independent atom model with screening corrected additivity rule (IAM –SCAR) method [35, 36]. Within the BEB framework, the cross sections for ionizing the i^{th} – orbital is giving by:

$$Q_i(t_i) = \frac{4\pi {a_o}^2 N_i}{t_i + u_i + 1} \left(\frac{R}{B_i}\right)^2 \left[\frac{\ln t_i}{2}\left(1 - \frac{1}{t_i^2}\right) + 1 - \frac{1}{t_i} - \frac{\ln t_i}{t_i + 1}\right]. \quad (3)$$

In equation (3) the binding energy of the ionized orbital B_i, is used to scale the electron impact energy (E_o) and orbital kinetic energy (U_i), $t_i = \frac{E_o}{B_i}$ and $u_i = \frac{U_i}{B_i}$, respectively. N_i is the orbital occupation number while R and a_o are, respectively, the Rydberg constant and Bohr radius. The BEB TICS is then obtained by summing up the contributions from each populated orbital.

To obtain the necessary molecule specific (*i. e.* for 1-propanol) information required for the calculation, quantum chemical calculations were performed in Gaussian 09 [37]. Here, the optimal 1-propanol geometry was first obtained at the B3LYP/aug-cc – pVDZ level. Single Point calculations were then performed using the Outer Valence Greens' function method and B3LYP levels, again with the aug-cc – pVDZ basis. Those calculations provide the ionization potentials and average orbital kinetic energies required to calculate the electron impact TICS within the BEB formalism. We note that this combination of quantum chemical calculation has yielded reasonable BEB TICS in our previous studies of small organic species [38 – 40]. In addition, Tanaka *et al.* [34] recently reviewed the efficacy of the BEB approach, for many atoms and molecules, and concluded that its TICS were usually accurate to better than 20% over an extended range of electron impact energies. We would anticipate a similar level of accord for 1 – propanol (see later). Two previous BEB results for 1-propanol, initially by Hudson *et al.* [14] and later updated by Bull *et al.* [23], are currently available in the literature. The TICS from Bull et al. supersedes that of Hudson *et al.*, and when we compare the present BEB TICS to that of Bull et al. [23] very good agreement (not shown) is found in spite of the fact that somewhat different quantum chemistries were employed in each case. As a consequence of this very good accord, neither of the earlier BEB results [14, 23] is considered any further in this paper.

As widely described in our previous papers [35, 36], the IAM-SCAR method is initially based on an optical potential calculation of electron scattering from the atoms constituting the molecular target of interest. The relevant scattering potential for each atom is represented as:

$$V(r) = V_{el}(r) + i\,V_{abs}(r), \qquad (4)$$

where $V_{el}(r)$ includes all the interaction terms corresponding to elastic scattering and the imaginary part, $V_{abs}(r)$, accounts for the inelastic processes which are considered as absorptions from the incident beam [41 – 43]. In this representation, an important parameter is the threshold energy above which the absorption potential applies*, i. e.* the first excited state of the atom in question. In this context, excitation to all the discrete and continuous energetically available states of the target are considered as a whole and therefore if we move this threshold energy up to the ionization limit, only ionizing collisions are included in the calculation procedure.

We used this approach to calculate the ionization cross sections of the atomic constituents of 1-propanol (*i.e.* C, O and H) and then we applied the SCAR procedure, as described in previous studies [44 - 46], to obtain the TICS for 1-propanol that we report here. At this stage we would characterise the TICS determined from the IAM-SCAR approach to be semi-phenomenological, so that we would not a priori expect its cross sections to be as accurate as those from the BEB

method. However, specific assessments of its efficacy should be made on a case by case basis and we return to this point shortly in our Results and Discussion section.

3. Results and Discussion

3.1 Mass Spectra and Cations Assignments

The absolute mass spectrum of cations generated from electron impact ionization of 1-propanol (C_3H_8O), using an incident electron of 70 eV, is shown in figure 1. Since the spectrometer analyzes the mass-to-charge ratio of fragments produced by interaction with electrons and all fragments appear in a single charged form, the measurements of the spectra can be interpreted as mass spectra. The mass resolution of our QMS allows us to separate adjacent peaks of 1 amu, as was demonstrated in our previous work reported in Ref. [9]. The present data compares quite well with the relative ratio intensities from NIST [28] and Macoll [47]. In this spectrum we observe the parent ion $C_3H_8O^+$(M), at mass 60 amu, and also more than 20 cationic fragments with an abundance higher than 1%. Our assignments for these fragments are listed in table 1, along with their relative abundances with respect to the base peak at m = 31 amu, their standard deviations and the percentage background contributions. The base peak assigned to the oxonium ion (CH_2O^+H), is the signature for primary alcohols and was also the main structure registered in our ethanol and methanol mass data as reported in Ref. [9]. It is observed that the intensity of the oxonium peak is remarkably bigger, constituting some 51% of the total ionization signal measured at that energy, in the 1-propanol mass spectrum when compared to the intensities of the other peaks registered, indicating that its formation is associated with the production of different fragmentation channels and the formation of different cations. That behavior was also observed for methanol and ethanol [9], however it was not so prominent there as in the present spectrum. This trend was not observed in our studies for butanol, that are to be published [48], meaning that the partial ionization cross section (PICS) for oxonium is not only a function of the size of the primary alcohol. Meanwhile, the relative intensity of the peak associated to the parent ion (m = 60 amu) compared to that for the oxonium ion, follows the same trend observed for ethanol and methanol. Namely, it is significantly smaller here than for ethanol, which was smaller than that for methanol [9]. This behavior indicates that the fragmentation is more spontaneous in the larger alcohols. There is some formation of H_3O^+ in the propanol spectrum, deviating from the tendency observed for methanol and propanol, given that the relative contribution of the H_3O^+ cations for propanol was smaller than that observed for methanol and ethanol in [9], but consistent with the observations from NIST [28]. We did not observe in our propanol spectrum that there was any production of CH_3OH^+, consistent with the study of Rejoub *et al.* [18]. We did, however, observe that the production of the CH_2O^+ cation decayed successively with an increase in the linear carbon chain length of the alcohols. In our mass spectrum (figure 1) we see a small intensity peak at mass 61 amu, which corresponds to the (M + 1) parent ion. This peak arises due to the natural isotope abundance of ^{13}C. Its intensity, measured with respect to that of the M cation (60 amu) is 3.8% to within the experimental uncertainties.

Besides oxonium, the next most abundant fragments observed are $C_2H_3^+$ (m = 27 amu) , $C_2H_4^+$(m = 28 amu), $C_2H_5^+$ or CHO^+(m = 29 amu), CH_4O^+(m = 32 amu), C_2HO^+(m = 41 amu), $C_2H_2O^+$ or $C_3H_6^+$ (m = 42 amu) , $C_3H_7O^+$(m = 59 amu) and $C_3H_8O^+$ (m = 60 amu). The parent cation $C_3H_8O^+$ is formed by the ejection of one of the lone-pair electrons from the oxygen atom, as these electrons have the lowest ionization energy (10.22 eV [33]). The group of cations observed in the mass spectrum between masses 52 - 59 amu, can be attributed to the sequential loss of a H atom from the parent ion. The peak at mass 46 amu is related to the formation of ionized ethanol, $C_2H_6O^+$, while the group of peaks seen between masses 40 - 45 amu are attributed to the sequential loss of a H atom from $C_2H_6O^+$. The masses between 43 – 36 amu are related to the ionized propyl radical ($C_3H_7^+$), and its subsequent sequential loss of a H atom. The peak at mass 33 amu is related to the formation of methyloxonium, CH_5O^+, with the group of peaks seen between masses 32-28 amu attributed to their sequential loss of a H atom. In addition, the masses between 30 – 24 amu are related to the ethane cation, $C_2H_6^+$, and its subsequent sequential loss of a H atom. We register a peak at mass 20 amu, with very small abundance, which is possibly due to the hydronium deuterated ion formation, H_2DO^+ (see table 1). The peaks observed at masses from 19 – 17 amu, 15 – 12 amu, 2 amu and 1 amu are assigned to the H_3O^+, H_2O^+, OH^+, CH_3^+, CH_2^+, CH^+, C^+, H_2^+ and H^+ cations, respectively.

3.2 Appearance Energies (AEs)

Although the Wannier law was originally developed for describing the near-threshold ionization of atoms, AEs for the various ionization processes and corresponding Wannier exponents may also be extracted from the experimental ionization yield curves for polyatomic molecules [29]. In this context, here we have recorded the ionization efficiency curves for the parent ion and for 31 of the fragment cations formed, and determined the corresponding appearance energies (AEs) from a near-threshold analysis for the 16 most intense peaks. This was achieved using the fitting procedure described in Section 2, with a couple of representative results from this process being given in figure 2.

The AEs we derived for those most prominant 16 cations within the mass spectrum, and their corresponding Wannier exponents, p, are listed in table 2, along with relevant values compiled by NIST [33] and Macoll [47]. The Wannier exponent is observed to vary between 1.34 and 3.23, and note that the AEs for cations with m = 44, 40, 30, 26, 12 amu have not been reported before. The parent ion of 1-propanol was found to have an AE value of 10.48 ± 0.01 eV, in good agreement with the values reported by NIST [33]. The other AEs we determined, as listed in table 2, are typically in excellent agreement with the values available from NIST. The exception to this general statement is the AE for $C_2H_3^+$ (m = 27 amu), registered at 13.42 ± 0.18 eV, which is 7.5% lower than the value reported at NIST [33]. Nonetheless they are still in pretty good agreement. As noted above, we report for the first time, to the best of our knowledge, new values of the AEs for the cations $C_2H_4O^+$ or $C_3H_8^+$ with m = 44 amu at 10.53 ±0.65 eV and 13.27±0.56 eV, for $C_3H_4^+$ or C_2O^+ with m = 40 amu at 10.45 ± 0.05 eV, for CH_2O^+ or $C_2H_6^+$ with m = 30

amu at 10.66 ±0.23 eV, for $C_2H_2^+$ with m = 26 amu at 10.99 ± 0.27 eV, and for C^+ with m = 12 amu at 22.32 ± 0.34 eV. Those AEs are found to be consistent, as a function of mass, with the values recorded for the other cations in the mass spectrum. In the determination of the AEs for mass 44 amu and 45 amu, in the fitting procedure we took into account that there were two different fragmentation channels available. For mass 44 amu, two different molecules could be produced, $C_3H_8^+$ or $C_2H_4O^+$, with the AEs being found at 10.53 eV and 13.27 eV, while for mass 45 amu two $C_2H_5O^+$ isomers may be formed, the methylmethylene oxonium species that has the oxygen ion located at the end of the carbon chain (CH_3-CH=O^+H) or methoxymethylium (CH_2=O^+-CH_3) where the oxygen ion is centered in the chain between two carbon atoms. The AEs for those cations were found to be at 11.33 eV and 13.03 eV, respectively. The higher value is most probably due the production of methoxymethylium, given that its formation involves a isomerisation of the molecule. Finally, note that in figure 2 we show results from our regular fitting procedure as applied in the determination of the AE for the parent ion (on the left), and from the modified fitting procedure to illustrate how the AE was determined for the production of $C_3H_8^+$ and $C_2H_4O^+$(on the right).

3.3 Ionization Cross Sections

Partial ionization cross sections (PICS) were measured for 32 cation masses of 1- propanol in the ranges 12 -15 amu, 24 - 33 amu, 36 - 45 amu and 53 - 60 amu, with a selection of those PICS, on an absolute scale, being given in figure 3. These masses constitute 96.6% of the cations generated by electron impact with 70eV electrons. The contribution of the cations O^+ or CH_4^+ , OH^+, H_2O^+, H_3O^+, H_2DO^+, $C_2H_6O^+$, C_3O^+, and $^{12}C_2{}^{13}CH_8O^+$ were excluded from the PICS obtained, as these ions constitute a small fraction (~2.7%) of the total ion yield collected. Furthermore, the PICS for H^+ and H_2^+, which constitute only 0.7% of the total ion yield, were also excluded from the absolute PICS we derived. Aside from their very small abundance, they were also excluded because it is extremely difficult to obtain accurate results for very light fragments using the mass spectrometer applied in this work [25, 9]. In addition, another reason for us not reporting PICS for H_2O^+ and OH^+ here is that their ionization efficiency curves contain a very high background contribution, 53.50% and 55.19% respectively. By summing the PICS for the 32 cations investigated, we obtained an estimation for the total ionization cross section (TICS) for 1-propanol. Recall that the present TICS and PICS were normalised to the absolute measurement of Rejoub *et al*. [18], as described before in Section 2. The current absolute TICS and PICS, for the 32 ions measured, are summarised in table 3, while figures 4 and 5 present our data compared to that available within the literature. Note that to our knowledge the PICS for the individual cations shown in figure 3 have not been reported previously, and so there are no independent experimental and theoretical cross sections against which we can compare them. All the PICS of figure 3 exhibit similar qualitative energy behavior, they are devoid of any structures although the rate of rise in the cross section magnitudes from threshold does vary for the different masses. The present TICS data in figure 4 are in quite good agreement with experimental data of Rejoub *et al.* [18] and our own Binary Encounter Bethe (BEB) calculation. A

minor exception to this, between our measured and BEB calculated TICS, is at energies above 60eV. This was expected, since our measured results somewhat underestimate the true TICS due to our omission of the contribution from the light cations. We also observe a lesser agreement with the other theoretical data (i.e. our IAM-SCAR result and the DM [14] result). While our IAM-SCAR calculation presents better qualitative agreement, it still overestimates the TICS for energies above 30 eV. On the other hand, the result from the DM calculation [14] significantly overestimates the magnitude of the cross section for energies above 40 eV. Note that there is a quite recent BEB result for the TICS from Bull *et al*. [23]. However, as that result is in very good accord with the present we do not plot it in figure 4. Figure 5 shows our PICS data compared to those of Rejoub *et al*. [18], for groups of masses. Due to the limited mass resolution of the Rejoub *et al.* [18] apparatus it was necessary to sum the cross section contribution for mass ranges of unresolved cations, in order to allow us to make a comparison with the only other data available in the literature. All of the PICS in figure 5 show similar characteristics to those in figure 3. Namely, a rapid 'turn on' from threshold followed by a quite uniform intensity for energies above about 40-50 eV. In this figure quite good agreement is seen between our results and those from Rejoub *et al.* [18], for the group of cations $C_2H_nO^+$ + $C_3H_n^+$ and CH_nO^+ + $C_2H_n^+$. However, it is also observed that the results from Rejoub *et al.* [18] overestimated our PICS for the ions labelled $C_3H_nO^+$, mainly for masses above 52 amu, although there is still quite good qualitative agreement between them in terms of the cross section shape and the appearance energy. The group of ions labelled CH_n^+ + H_nO^+ contain ions with masses from 12-15 amu in the present data, and from 12-19 amu for the Rejoub *et al.* [18] data. It was expected therefore, that the PICS from Rejoub *et al.* [18] would be higher in magnitude than ours, given that it includes more cations (HO^+, H_2O^+ and H_3O^+, O^+ and CH_4^+). To evaluate the contribution of those "missing" cations in our data, although we did not specifically measure their PICS, we employ the mass spectrum we obtained at 70 eV. From that spectrum, at that energy, we can account for the cross sections of the "missing" cations and on doing so we obtain a revised value of 0.51 x 10^{-16} cm^2. This value is also plotted in figure 5, where we find it is in much better accord with the Rejoub *et al*. [18] result when the errors are accounted for.

4. Conclusions

This work reported on measurements of the cation mass spectra, ionization efficiency curves, and a determination of the appearance energies and Wannier exponents for electron impact on 1-propanol molecules. We detected 41 well-resolved mass peaks, from 1-61 amu mass range, in the mass spectrum and determined their identity and abundance. The present mass spectrum was found to be in good agreement with the earlier data reported by NIST [28] and Macoll [47]. Original partial ionization cross section data for the 32 most intense cations were reported over the 10 - 100 eV range, while our total ionization cross sections were compared with the experimental data of Rejoub *et al.* [18] and the theoretical Binary-Encounter-Bethe (BEB), IAM-SCAR and semi-classical Deutsch-Märk (DM) results [11]. We observed a good overall agreement between our present

measured data and theoretical results (i.e. our BEB calculations) and with the Rejoub *et al*. TICS [18].

Agreement with the IAM-SCAR and DM computations was less satisfactory, although the IAM-SCAR did qualitatively reproduce the experimental results over the common energy range. Finally, the appearance energies and Wannier exponents of the identified cations were also determined in this study, and found to be in generally fair accord with the NIST sourced data. The importance of absolute ionization cross section results, such as contained in this paper, can be clearly appreciated from the recent papers from Ridenti *et al*. [49] and Brunger [50], and we refer the interested reader to those publications for further details.

Acknowledgements

M.C.A.L. acknowledges financial support from CNPq, FAPEMIG and FINEP, while M.J.B. thanks CNPq for his "Special Visiting Professor" award. K.L.N. thanks CNPq for an "Attracting Young Talent Grant" under the "Science Without Borders" program. Some financial assistance from the Australian Research Council is also noted. Finally, S. Ghosh acknowledges for his grant from PNPD/CAPES while G Garcia thanks the Spanish Ministerio de Economia, Industria y Competitividad for his project grant FIS 2016 -80440 and the EU project FP7 – ITN – ARGENT - 608163.

References

[1] A. K. Agarwal, Progress in Energy and Combustion Science 33 (2007) 2007.
[2] S. Payne, T. Dutzik and E. Figdor, Environment America Research and Policy Center (2009). http://www.environmentamerica.org/sites/environment/files/reports/The-High-Cost- of-Fossil-Fuels.pdf.
[3] B. Pieprzyk, N. Kortlüke and P. R. Hilje, The impact of fossil fuels. Greenhouse gas emissions, environmental consequences and socio-economic effects, Energy Research Architecture Report (2009) 225. http://www.bee-ev.de/_ downloads/.
[4] A. Demirbas, Energy Policy 35 (2007) 4661.
[5] M. Mofijur, M. G. Rasul and J. Hyde, Procedia Engineering 105 (2015) 658.
[6] S. Brusca, R. Lanzafame, A. M. Garrano and M. Messina, Energy Procedia 45 (2014) 889.
[7] S. Pischinger, Topics in Catalysis 59 (2016) 834.
[8] S. M. Starikovskaia, J. Phys. D: Appl. Phys .39 (2006) R265.
[9] K. L. Nixon, W. A. D. Pires, R. F. C. Neves, H. V. Duque, D. B. Jones, M. J. Brunger and M. C. A. Lopes, Int. J. Mass. Spectrom. 404 (2016) 48.
[10] M. J. Brunger and S. J. Buckman, Phys. Reports 357 (2002) 215.
[11] H. Deutsch, K. Becker, R. Basner, M. Schmidt and T. D. Märk, J. Phys. Chem. A 102 (1998) 8819.
[12] M. Vinodkumar, K. Korot and P. C. Vinodkumar, Int. J. Mass. Spectrom. 305 (2011) 26 .
[13] N. Duric, I. Cadez, and M.V. Kurepa, Fizika 21 (1989), 339
[14] J. E. Hudson, M. L. Hamilton, C. Vallance and P. W. Harland, Phys. Chem. Chem. Phys. 5 (2003) 3162.
[15] S. Pal, Chem. Phys. 302 (2004) 119.
[16] S. K. Srivastava, E. Krishnakumar, A. F. Fucaloro and T. van Note, J. Geophys. Res. 101 (1996) 26155.
[17] K. M. Douglas and S. D. Price, J. Chem. Phys. 131 (2009) 224305.
[18] R. Rejoub, C. D. Morton, B. G. Lindsay and R. F. Stebbings , J. Chem. Phys. 118 (2003) 1756.
[19] A. N. Zavilopulo, F. F. Chipev, L. M. Kokhtych, Nucl. Instrum. Methods Phys. Res. B 233 (2005) 302.
[20] C. S. Cummings, W. Bleakney, Phys. Rev. 58 (1940) 787.
[21] M. A. Khakoo, J. Muse, H. Silva, M. C. A. Lopes, C. Winstead, V. McKoy, E. M. de Oliveira, R. F. da Costa, M. T. do N. Varella, M. H. F. Bettega, and M. A. P. Lima, Phys. Rev. A 78 (2008) 062714.
[22] J. M. Williams and W. H. Hamill, J. Chem. Phys. 49 (1968) 4467.
[23] J. N. Bull, P. W. Harland and C. Vallance, J. Phys. Chem. A 116 (2012) 767.
[24] T. Takeuchi, S. Ueno, M. Yamamoto, Int. J. Mass. Spectrom 64 (1985) 33.
[25] Hiden Analytical: http://www.hidenanalytical.com/en/.
[26] R. Rejoub, B. G. Lindsay and R. F. Stebbings, Phys. Rev. A 65 (2002) 042713.
[27] MDC Vacuum Products, http://www.mdcvacuum.com.
[28] NIST Webook: http://webbook.nist.gov/cgi/inchi?ID=C71238&Mask=4&Type=ANTOINE&Plot=on
[29] T. Fiegele, G. Hanel, I. Torres, M. Lezius and T. D. Märk, J. Phys. B 33 (2000) 4263.
[30] S. Denifl, B. Sonnweber, G. Hanel, P. Scheier, T. D. Märk, Int. J. Mass. Spectrom. 238 (2004) 47.
[31] P. R. Bevington 'Data reduction and error analysis for the physical sciences' McGraw – Hill, New York (1969).
[32] B. Gstir, S. Denifj, G. Hanel, M. Rümmele, T. Fiegele, P. Cicman, M. Stano, S. Matejcik, P.Scheier, K. Becker A. Stamativic and T. D. Märk, J. Phys. B: At. Mol. Opt. Phys. 35 (2002) 2993
[33] NIST web book: http://webbook.nist.gov/cgi/inchi?ID=C71238&Mask=20#ref-16.
[34] H. Tanaka, M. J. Brunger, L. Campbell, H. Kato, M. Hoshino and A. R. P. Rau, Rev. Mod. Phys., 88 (2016) 025004.
[35] F. Blanco and G. Garcia, J. Phys. B 42 (2009) 145203.
[36] O. Zatsarinny, K. Bartschat, G. Garcia, F. Blanco, L. R. Hargreaves, D. B. Jones, R. Murrie, J. R. Brunton, M. J. Brunger, M. Hoshino and S. J. Buckman, Phys. Rev. A 83 (2011) 042702.
[37] M. J. Frisch et al., Gaussian 09, Revision B.01 (2010).
[38] H. V. Duque, L. Chiari, D. B. Jones, P. A. Thorn, Z. Pettifer, G. B. da Silva, P. Limão-Vieira, D. Duflot, M. J. Hubin-Franskin, J. Delwiche, F. Blanco, G. Garcia, M. C. A. Lopes, K. Ratnavelu, R. D. White and M. J. Brunger, Chem. Phys. Letts 608 (2014) 161.
[39] D. B. Jones, R. F. da Costa, M. T. do N. Varella, M. H. F. Bettega, M. A. P. Lima, F. Blanco, G. Garcia and M. J. Brunger, J. Chem. Phys. 144 (2016) 144303.
[40] R. F da Costa, E. M. de Oliveira, M. H. F. Bettega, M. T. do N. Varella, D. B. Jones, M. J. Brunger, F.

Blanco, R. Colmenares, P. Limão-Vieira, G. Garcia and M. A. P. Lima, J. Chem. Phys. 142 (2015) 104304.
[41] M. E. Riley and D. G. Truhlar, J. Chem. Phys. 63 (1975) 2182.
[42] X. Zhang, J. Sun and Y. Liu, J. Phys. B 25 (1992) 1893.
[43] G. Staszewska, D. W. Schwenke, D. Thirumali and D. G. Truhlar, Phys. Rev. A 28 (1983) 2740.
[44] F. Blanco and G. Garcia, Phys. Lett. A 317 (2003) 458.
[45] F. Blanco and G. Garcia, Phys. Lett. A 330 (2004) 230.
[46] F. Blanco, L. Ellis-Gibbings and G. Garcia, Chem. Phys. Lett. 645 (2016) 71.
[47] A. Macoll, Org. Mass Spectrom. 21 (1986) 601.
[48] W. A. D. Pires, K. L. Nixon, S. Ghosh, R. R. dos Santos, R. F. C. Neves, R. A. A. Amorin, H. V. Duque, D. B. Jones, G. Garcia, M. J. Brunger and M. C. A. Lopes, Int. J. Mass. Spectrom *(to be submitted).*
[49] M. A. Ridenti, J. A. Filho, M. J. Brunger, R. F. da Costa, M. T. do N. Varella, M. H. F. Bettega and M. A. P. Lima, Eur. Phys J D 70 (2016) 161.
[50] M. J. Brunger, Int. Rev. Phys. Chem. 36 (2017) 333.

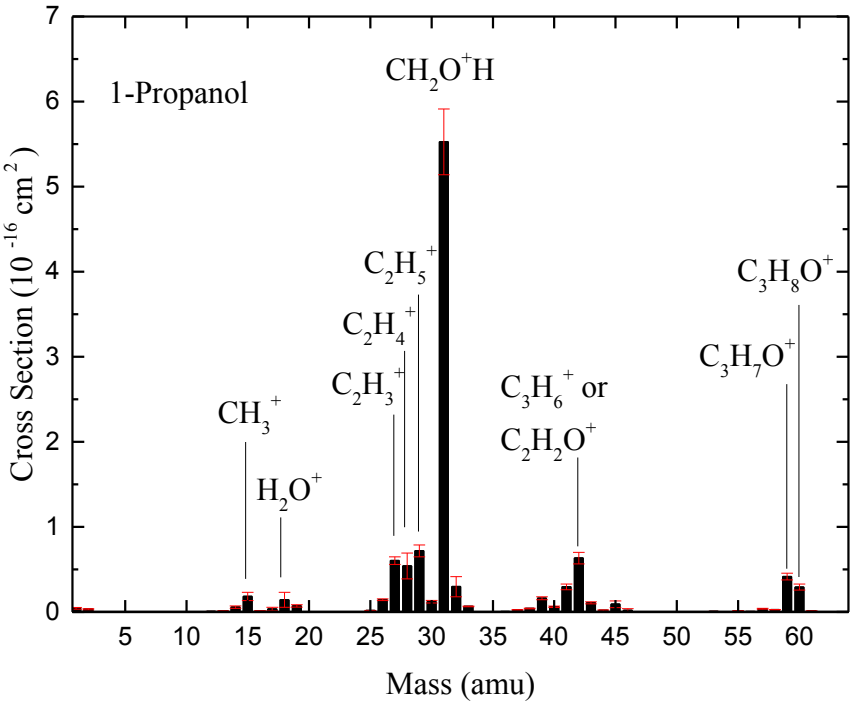

Fig. 1. Mass spectrum of the cations produced by 70 eV electron impact ionization of 1-propanol. Note that in this spectrum the value of the ratio m/z, which is the parameter detected by the mass spectrometer, is equal to the value of the mass, given that all the cations detected here are singly ionized. The spectrum is placed on an absolute scale through normalisation to the absolute measurement of Rejoub *et al*. [18]. Note that here the background spectrum was previously subtracted from the signal plus background spectrum. The error bars represent the mean square root of the square of the statistical error on our measurements, added to the square of the total error on the Rejoub *et al*. [18] cross sections.

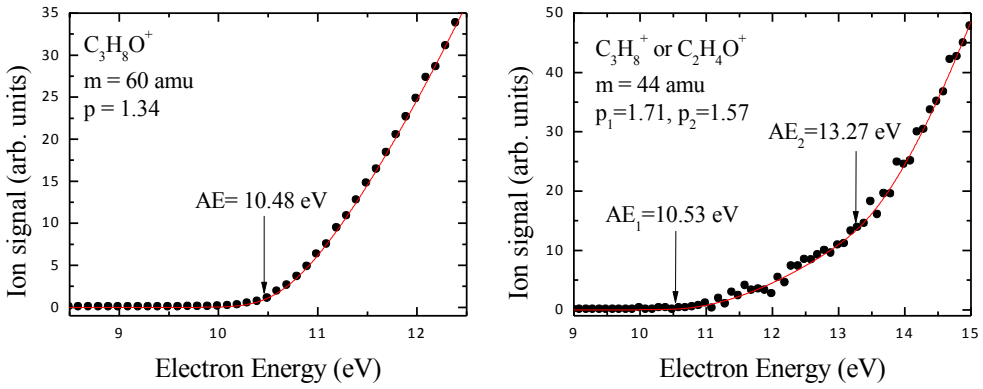

Fig. 2. Results from the fitting procedure applied in the determination of the AEs from the experimental ionization efficiency curves of electron ionization on 1-propanol, near-threshold. The AEs are indicated by arrows, while the solid line shows the exponential functions fitted to our experimental data as registered for the parent ion (left) and mass = 44 amu (right) corresponding to $C_3H_8^+$ or $C_2H_4O^+$.

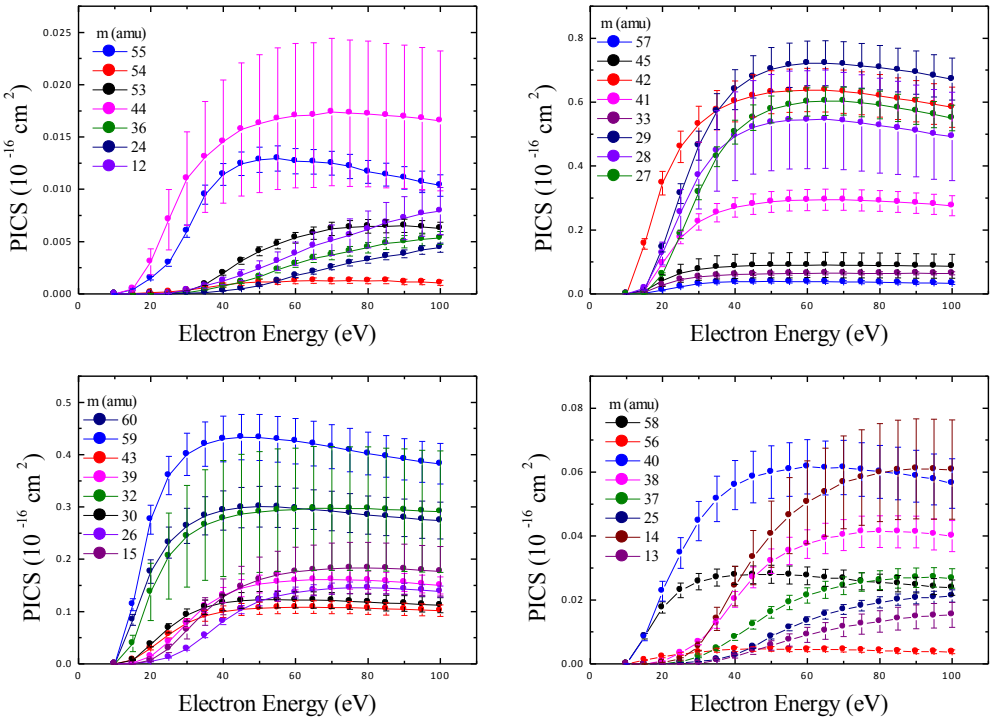

Fig. 3. Absolute partial ionization cross sections (PICS) for 31 of the 32 cations that result from electron impact ionization of 1-propanol, as measured in the present study. The errors are the quadrature sum of (i) the uncertainty in the experimental measurements of the cross sections, (ii) the uncertainty of the relative contributions to the mass spectrum and (iii) the normalization to the absolute data of Rejoub *et al*. [18]. In the various legends the cations are labelled in terms of their m/z, see text and table 1 for their formulae. Finally we note that the lines through the various data points here have no physical meaning, they are simply there to guide the reader's eye.

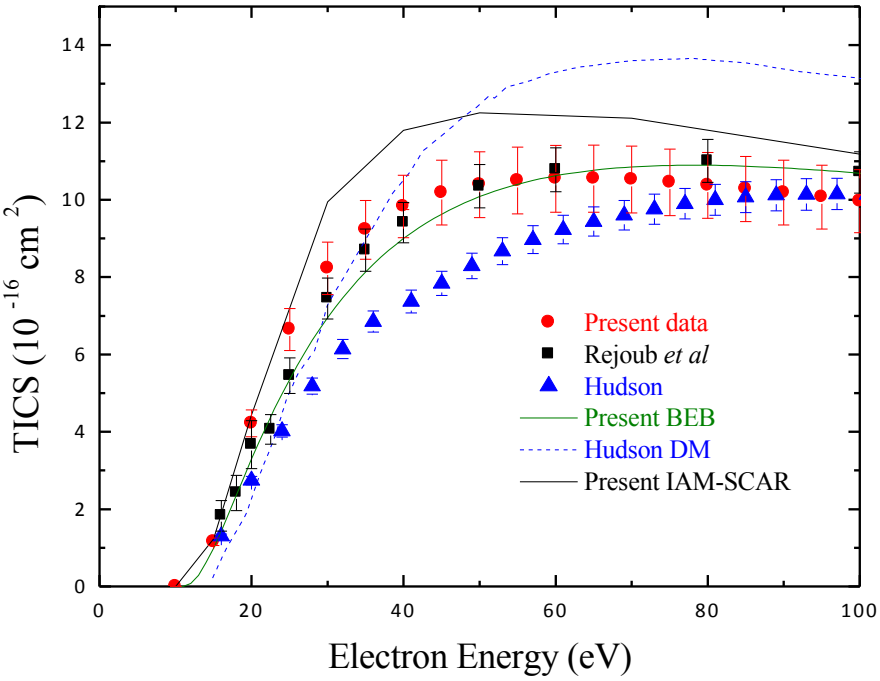

Fig. 4. Total ionization cross section for electron scattering from 1-propanol as obtained in this work, both experimental and theoretical, compared to data from other theoretical and experimental studies. Our experimental TICSs were obtained by taking into account the sum of 32 cations, representing 96.6 % of the cations measured within the mass spectrum. See also legend on figure and text for further details.

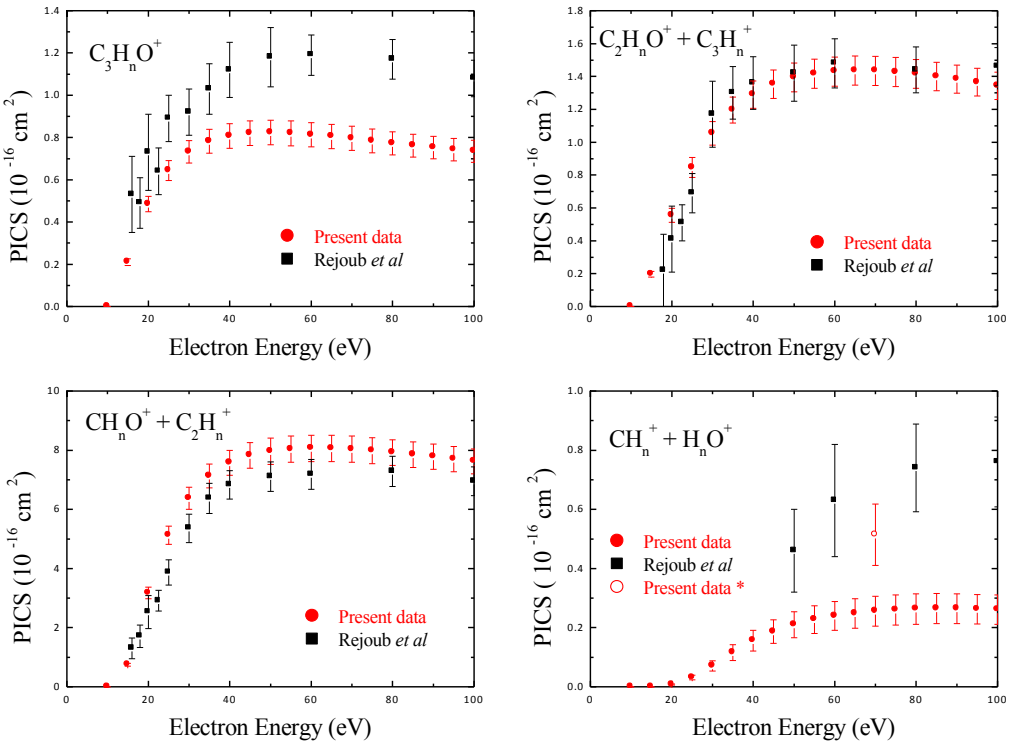

Fig. 5. Absolute partial ionization cross sections (PICS) for cations grouped within similar masses m, to enable comparison with the data from Rejoub *et al.* [18] . Here $C_3H_nO^+$ represents cations with m = 60-52 amu, $C_2H_nO^+ + C_3H_n{}'^+$ are cations with m = 46-36 amu, $CH_nO^+ + C_2H_n{}'^+$ are cations with m = 33-24 amu and $CH_n^+ + H_n{}'O^+$ are cations with m = 15-12 amu, according to table 1. The datum labelled as *Present data**, was obtained including the signal registered for cations with a high background signal and therefore a high uncertainty, as discussed in the paper.

Table 1: Relative abundances of the cations generated by electron impact of 1-propanol using an electron energy of 70 eV. The relative abundance is expressed with respect to the most abundant cation, *i.e.* 31 amu. The present data are determined from the average of several measurements and the error is the standard deviation on that average. Also shown is the background contribution to measurements of 1-propanol, given as a percentage. The data from this study are compared with the corresponding results from other sources.

Cation Identity	**m (amu)**	**Present Data**			**NIST[33]**	**Macoll [47]**
		Abundance	Error	% Background		
H^+	1	0.77	0.12	35.05		
H_2^+	2	0.58	0.07	23.57		
C^+	12	0.09	0.02	2.47		0.19
CH^+	13	0.21	0.03	0.82	0.23	0.44
CH_2^+	14	1.03	0.16	2.65	0.83	1.87
CH_3^+	15	3.30	0.57	1.12	2.45	5.23
O^+ or CH_4^+	16	0.21	0.06	18.35	0.1	0.38
OH^+	17	0.62	0.34	53.50		1.27
H_2O^+	18	2.58	1.50	55.19	0.3	4.20
H_3O^+	19	1.27	0.06	0.72	0.82	1.36
H_2DO^+	20	0.05	0.00	15.49		0.09
C_2^+	24	0.05	0.00	0.59	0.17	0.10
C_2H^+	25	0.31	0.02	0.56	0.81	0.52
$C_2H_2^+$	26	2.61	0.07	0.40	5.52	4.68
$C_2H_3^+$	27	10.91	0.22	0.50	16.28	16.28
CO^+ or $C_2H_4^+$	28	9.79	2.66	5.38	6.43	7.50
COH^+ or $C_2H_5^+$	29	13.00	0.88	0.73	17.66	15.29
CH_2O^+ or $C_2H_6^+$	30	2.19	0.23	0.24	0.1	2.30
CH_3O^+	31	100	0.00	0.04	100	100
CH_4O^+	32	5.38	2.11	2.30	1.95	2.63
CH_5O^+	33	1.17	0.03	0.05	1.09	1.16
C_3^+	36	0.07	0.00	1.72	0.27	0.02
C_3H^+	37	0.44	0.02	0.48	1.22	0.75
$C_3H_2^+$	38	0.73	0.05	0.66	1.86	1.16
$C_3H_3^+$	39	2.92	0.13	1.18	6.58	3.96
C_2O^+ or $C_3H_4^+$	40	1.11	0.10	1.23	1.43	0.85
C_2HO^+ or $C_3H_5^+$	41	5.33	0.27	2.52	8.54	5.61
$C_2H_2O^+$ or $C_3H_6^+$	42	11.45	0.4	0.30	13.5	8.56
$C_2H_3O^+$ or $C_3H_7^+$	43	1.95	0.09	6.97	4.04	2.90
$C_2H_4O^+$ or $C_3H_8^+$	44	0.31	0.12	9.33	0.72	0.45
$C_2H_5O^+$	45	1.63	0.69	0.48	1.64	1.22
$C_2H_6O^+$	46	0.33	0.35	0.43		
C_3O^+	52	0.02	0.00	24.35		
C_3HO^+	53	0.11	0.00	7.06	0.26	0.09
$C_3H_2O^+$	54	0.02	0.00	25.17		
$C_3H_3O^+$	55	0.23	0.01	28.73	0.51	0.32
$C_3H_4O^+$	56	0.08	0.01	34.50		
$C_3H_5O^+$	57	0.68	0.06	18.42	0.98	0.79
$C_3H_6O^+$	58	0.48	0.02	1.67		0.13
$C_3H_7O^+$	59	7.51	0.39	0.06	10.93	8.12
$C_3H_8O^+$	60	5.20	0.50	0.06	6.64	4.34
$^{12}C_2{}^{13}CH_8O^+$	61	0.20	0.02	0.20		

Table 2: Appearance energies and Wannier exponents p, determined for some of the ions of 1-propanol (in eV) that are formed by electron impact.

m (amu)	**NIST[33]**	**Present Data**	***p***
60	10.22 ± 0.07[a]	10.48±0.01	1.34
	10.15 ± 0.025[b]		
	10.32 ± 0.02[c]		
59	10.72 ± 0.09[a]	10.76±0.02	1.74
	10.48 ± 0.03[b]		
	10.72[d]		
	10.2[e]		
	10.69[f]		
45	11.35 ± 0.04[g]	11.33±0.42	1.51
	11.1 ± 0.1[d]	13.03±0.17	1.27
	11.1[h]		
44	-	10.53±0.65	1.71
		13.27±0.56	1.57
43	11.6 ± 0.1[d]	10.59±0.05	1.45
42	10.56 ± 0.05[i]	10.62±0.01	1.41
	10.65 ± 0.09[a]		
	10.3[e]		
	10.33 ± 0.03[b]		
	10.65 ± 0.03[d]		
41	12.6[d]	11.84±0.15	2.70
40	-	10.45±0.05	1.54
39	15.6[h]	11.44±0.16	1.98
31	11.20[j]	11.60±0.02	2.10
	12.3 ± 0.9[a]		
	11.50 ± 0.08[k]		
	11.16 ± 0.03[b]		
	~11.3[d]		
	~11.11[l]		
30	-	10.66±0.23	3.04
29	12.3[d]	12.26±0.06	2.50
28	~11.9[d]	11.33±0.11	2.64
27	14.7[h]	13.42±0.18	3.23
26	-	10.99±0.27	2.55
12	-	22.32±0.34	1.55

a. Bowen, R.D.; Maccoll, A. Org. Mass Spectrom.1984, 19, 379.
b. Johnstone, R.A.W .; Mellon, F. A., J. Chem. Soe. Faraday Trans. 2, 1972, 68, 1209.
c. Cocksey, B.J.; Eland, J.H.D.; Danby, C.J., J. Chem. Soc., 1971, (B), 790.
d. Refaey, K.M.A.; Chupka, W.A., J. Chem. Phys., 1968, 48, 5205.
e. McLafferty, F.W.; Bente, P.F., III; Kornfeld, R.; Tsai, S.-C.; Howe, I., J. Am. Chem. Soc., 1973, 95, 2120.
f. Lambdin, W.J.; Tuffly, B.L.; Yarborough, V.A., Appl. Spectry., 1959, 13, 71.
g. Solka, B.H.; Russell, M.E., J. Phys. Chem., 1974, 78, 1268..
h. Friedman, L.; Long, F.A.; Wolfsberg, M., J. Chem. Phys., 1957, 27, 613.
i. Holmes, J.L.; Mommers, A.A.; Szulejko, J.E.; Terlouw, J.K., J. Chem. Soc., Chem. Commun., 1984, 165..
j. Holmes, J.L.; Lossing, F.P.; Maccoll, A., J. Am. Chem. Soc., 1988, 110, 7339.
k. Selim, E.T.M.; Helal, A.I., Indian J. Pure Appl. Phys., 1981, 19, 977.
l. Chupka, W.A., J. Chem. Phys., 1959, 30, 191.